Supplementary Information

Tailoring Atomically Dispersed Fe-Induced Oxygen Vacancy for Highly Efficient Gas-Phase Photocatalytic CO_2 Reduction and NO Removal with Diminished Noxious Byproducts

Nguyen Quoc Thang [1, 2, 3, 4, 5], Amr Sabbah [2, 6, 7, *], Chih-Yang Huang [2, 8, 9], Nguyen Hoang Phuong [10], Tsai-Yu Lin [2, 8, 9], Mahmoud Kamal Hussien [1, 2, 11], Heng-Liang Wu [2, 6, 12], Chih-I Wu [13], Nguyet N. T. Pham [14], Pham Van Viet [10], Chih-Hao Lee [5], Li-Chyong Chen [2, 6, 15, *], Kuei-Hsien Chen [1, 2, *]

[1] Institute of Atomic and Molecular Sciences, Academia Sinica, Taipei 10617, Taiwan

[2] Center for Condensed Matter Sciences, National Taiwan University, Taipei 10617, Taiwan

[3] Nano Science and Technology Program, Taiwan International Graduate Program, Academia Sinica, Taipei 115, Taiwan and National Tsing Hua University, Hsinchu, 300, Taiwan

[4] Institute of Physics, Academia Sinica, Taipei 15201, Taiwan

[5] Department of Engineering and System Science, National Tsing Hua University, Hsinchu, 30013, Taiwan

[6] Center of Atomic Initiative for New Materials, National Taiwan University, Taipei, 106, Taiwan

[7] Tabbin Institute for Metallurgical Studies, Tabbin, Helwan 109, Cairo 11421, Egypt

[8] International Graduate Program of Molecular Science and Technology, National Taiwan University (NTU-MST), Taipei 10617, Taiwan

[9] Molecular Science and Technology Program, Taiwan International Graduate Program (TIGP), Academia Sincia, Taipei 11529, Taiwan

[10] Advanced Materials and Applications Research Group, Ho Chi Minh University of Technology, 475A Dien Bien Phu Street, Binh Thanh District, Ho Chi Minh City 700000, Vietnam

[11] Department of Chemistry, Faculty of Science, Assiut University, Assiut 71516, Egypt

[12] Department of Chemistry, National Taiwan University, Taipei 10617, Taiwan

[13] Graduate Institute of Photonics and Optoelectronics, National Taiwan University, Taipei 10617, Taiwan

[14] Faculty of Chemistry, University of Science, Vietnam National University Ho Chi Minh City, Ho Chi Minh 700000, Vietnam.

[15] Department of Physics, National Taiwan University, Taipei 10617, Taiwan

*Corresponding author: chenkh@pub.iams.sinica.edu.tw (K.-H. Chen)

chenlc@ntu.edu.tw (L.-C. Chen)

amrsabbah@ntu.edu.tw (A. Sabbah)

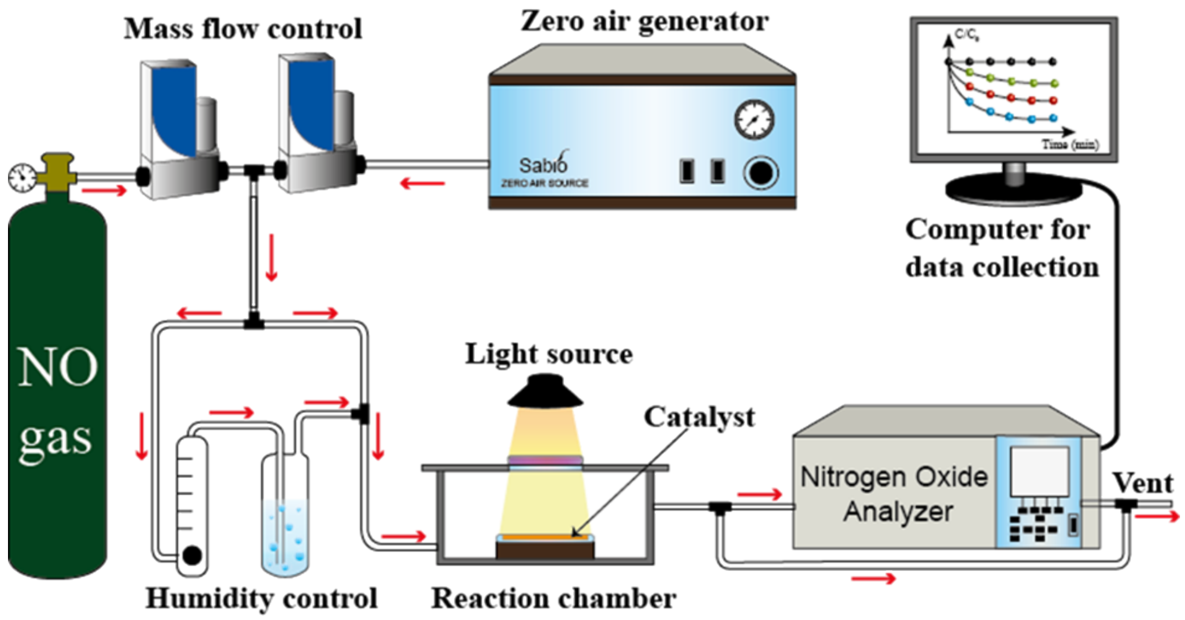

Figure S1. Schematic illustration of photocatalytic NO removal setup.

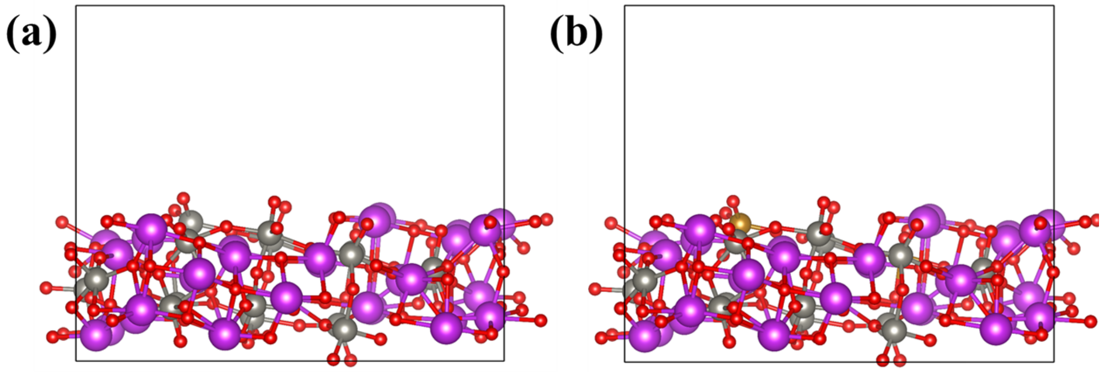

Figure S2. The most optimized configuration of **(a)** pristine Bi_2WO_6 (131) and **(b)** Fe-Bi_2WO_6 (131). The grey, pink, red, and deep yellow spheres represent tungsten (W), bismuth (Bi), oxygen (O), and iron (Fe), respectively.

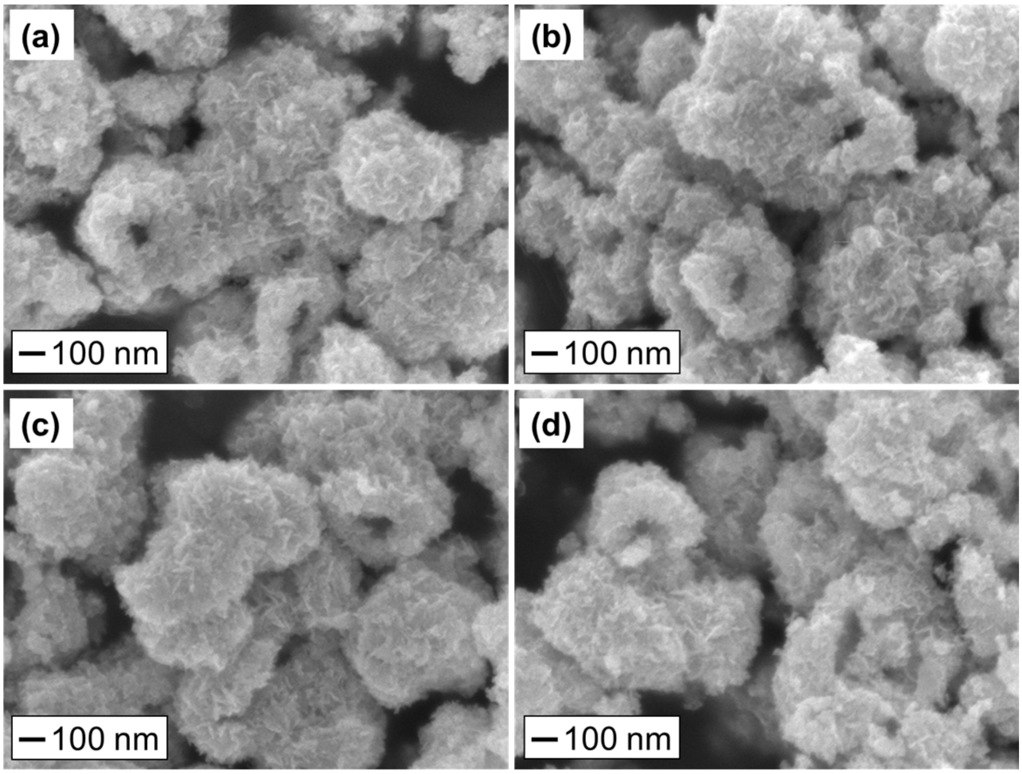

Figure S3. SEM images of **(a)** pristine Bi_2WO_6, and **(b-d)** xFe-Bi_2WO_6 where x = 1, 1.5, 2, respectively.

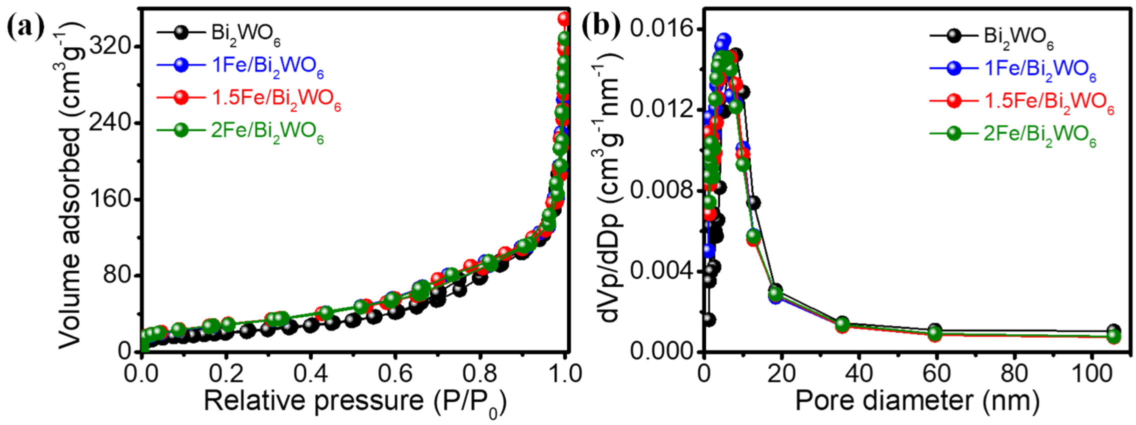

Figure S4. (a) Nitrogen adsorption-desorption isotherms, and **(b)** pore size distribution of Bi_2WO_6 and xFe-Bi_2WO_6 (x = 1, 1.5, 2).

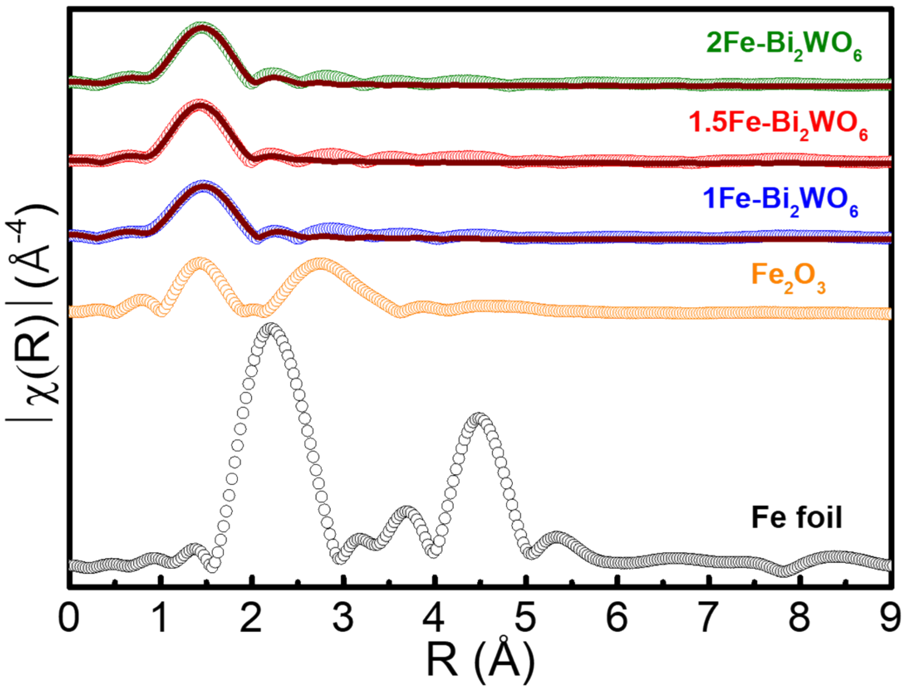

Figure S5. Fourier-transform extended X-ray absorption fine structure (FT-EXAFS) fitting curves of xFe-Bi_2WO_6 (x = 1, 1.5, 2) and FT-EXAFS curves of Fe foil and Fe_2O_3.

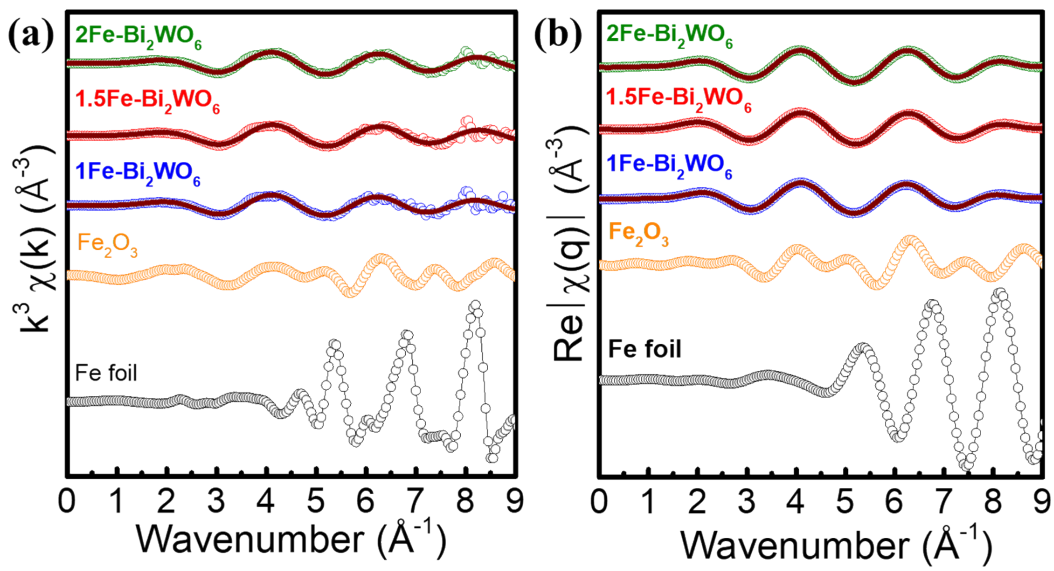

Figure S6. Fourier transform of Fe K-edge EXAFS spectra in **(a)** k, and **(b)** q space for Fe foil, Fe_2O_3, and the corresponding fitting curves for xFe-Bi_2WO_6 (x=1, 1.5, 2).

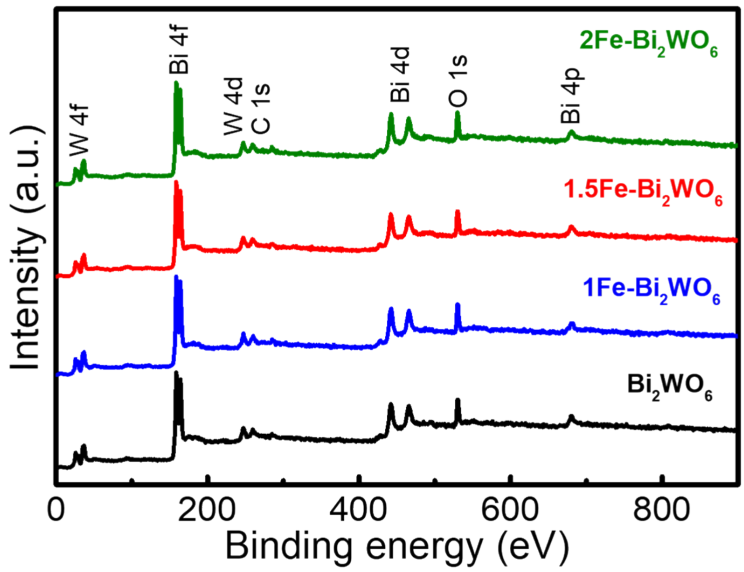

Figure S7. XPS survey spectra of Bi_2WO_6 and xFe-Bi_2WO_6 (x=1, 1.5, 2).

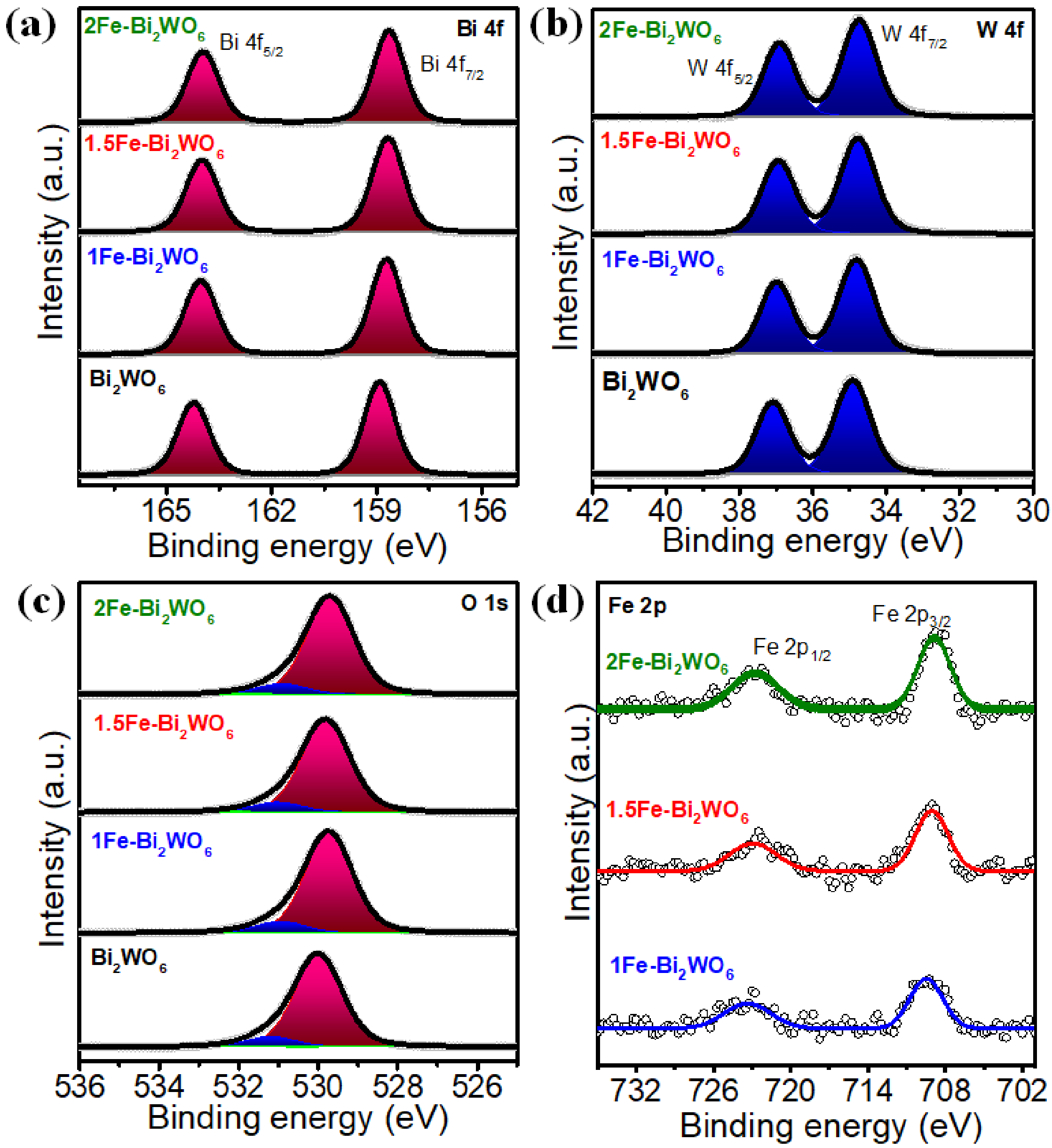

Figure S8. High-resolution X-ray photoelectron spectra of Bi_2WO_6, and xFe-Bi_2WO_6 (x=1, 1.5, 2).

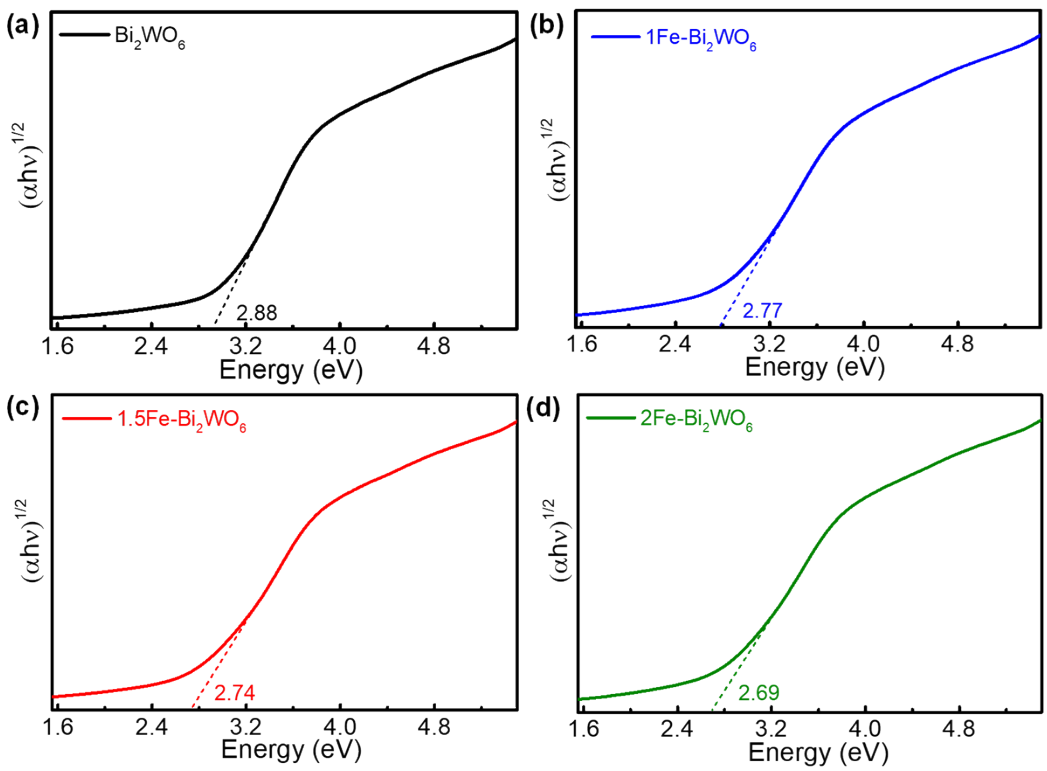

Figure S9. Tauc plots for Bi_2WO_6 and xFe-Bi_2WO_6 (x=1, 1.5, 2).

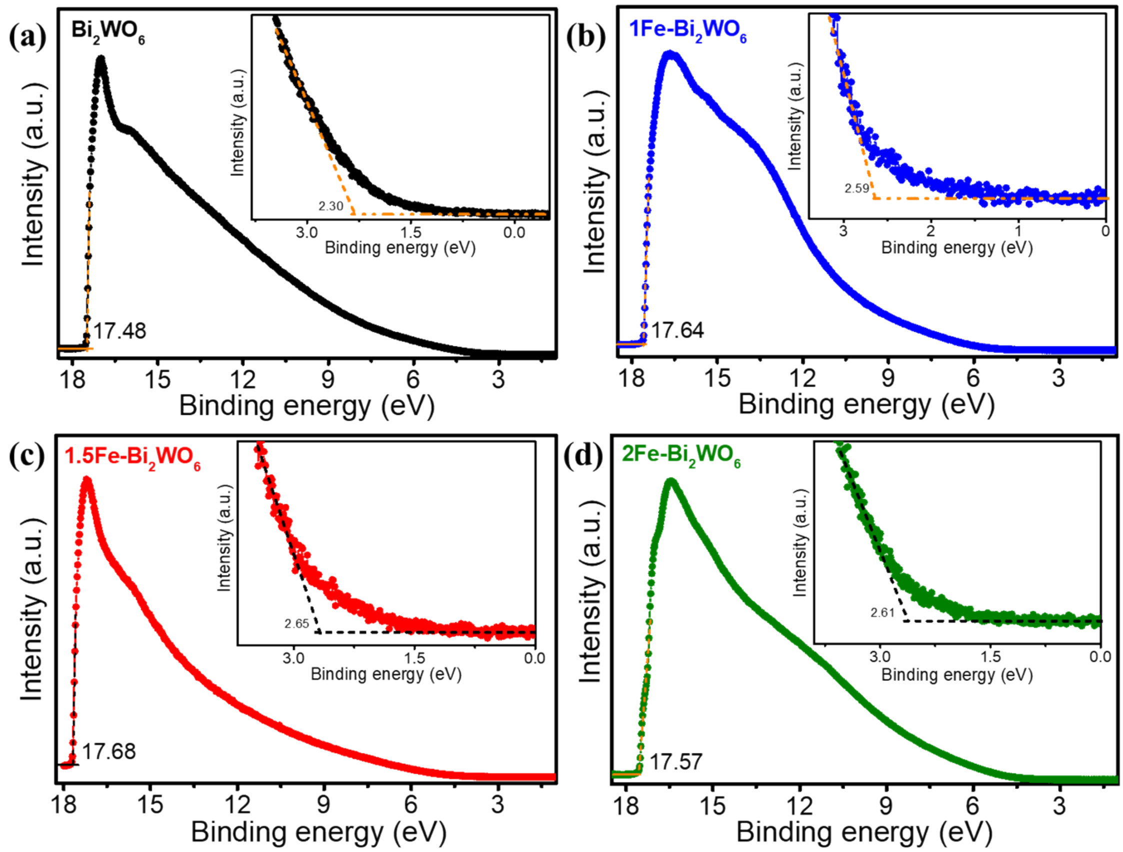

Figure S10. UPS spectra of Bi_2WO_6 and xFe-Bi_2WO_6 (x=1, 1.5, 2).

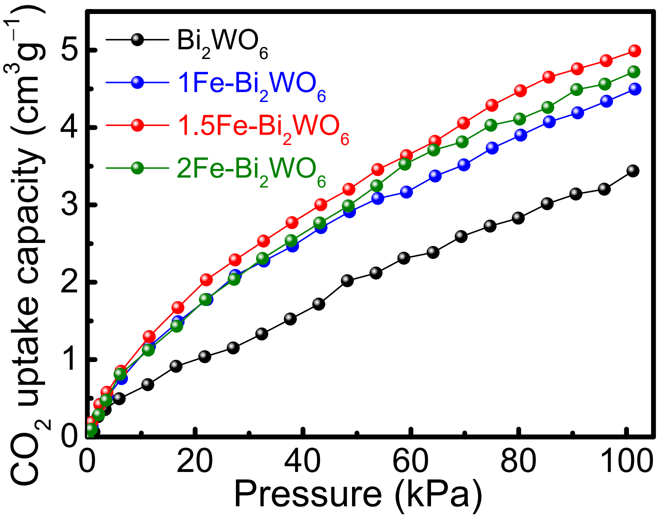

Figure S11. CO_2 adsorption curves for Bi_2WO_6 and $xFe-Bi_2WO_6$.

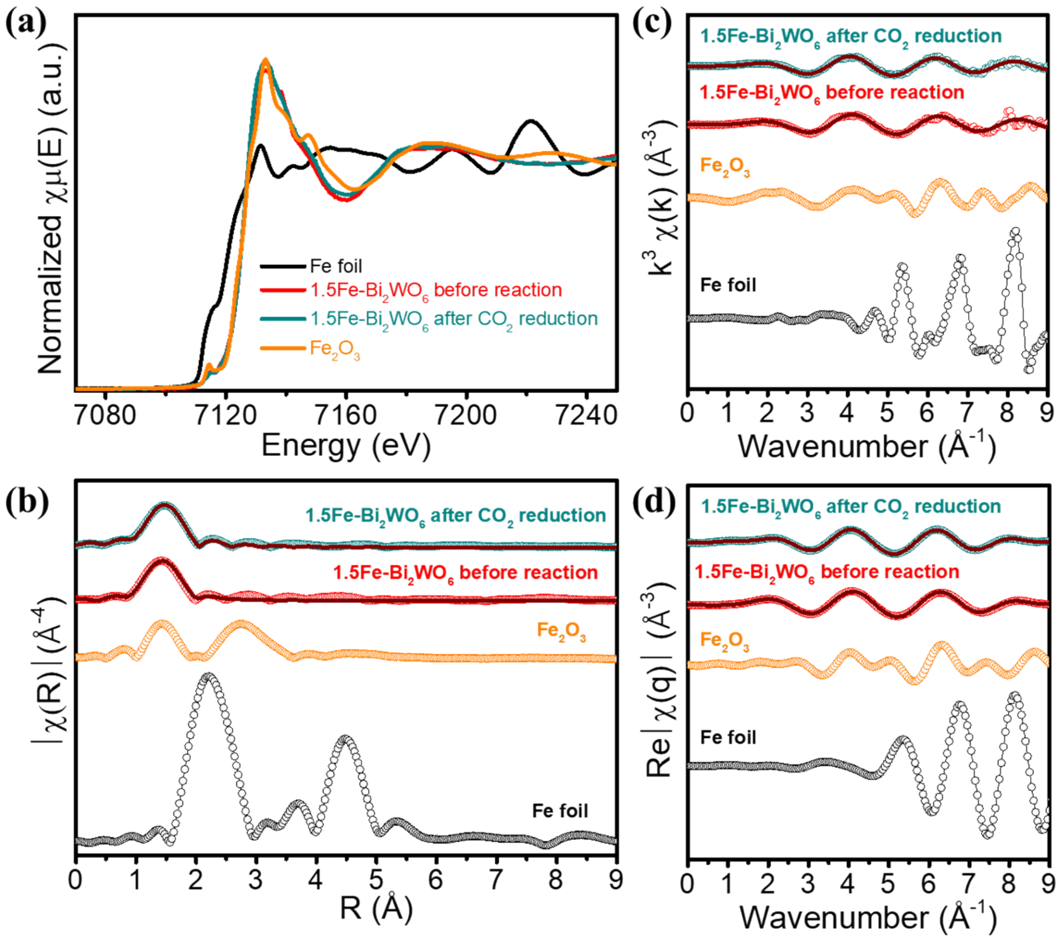

Figure S12. (a) Fe K-edge XANES, **(b-d)** FT-EXAFS spectra and corresponding fitting curves of Fe foil, Fe_2O_3, and 1.5Fe-Bi_2WO_6 before and after stability test for photocatalytic CO_2 reduction.

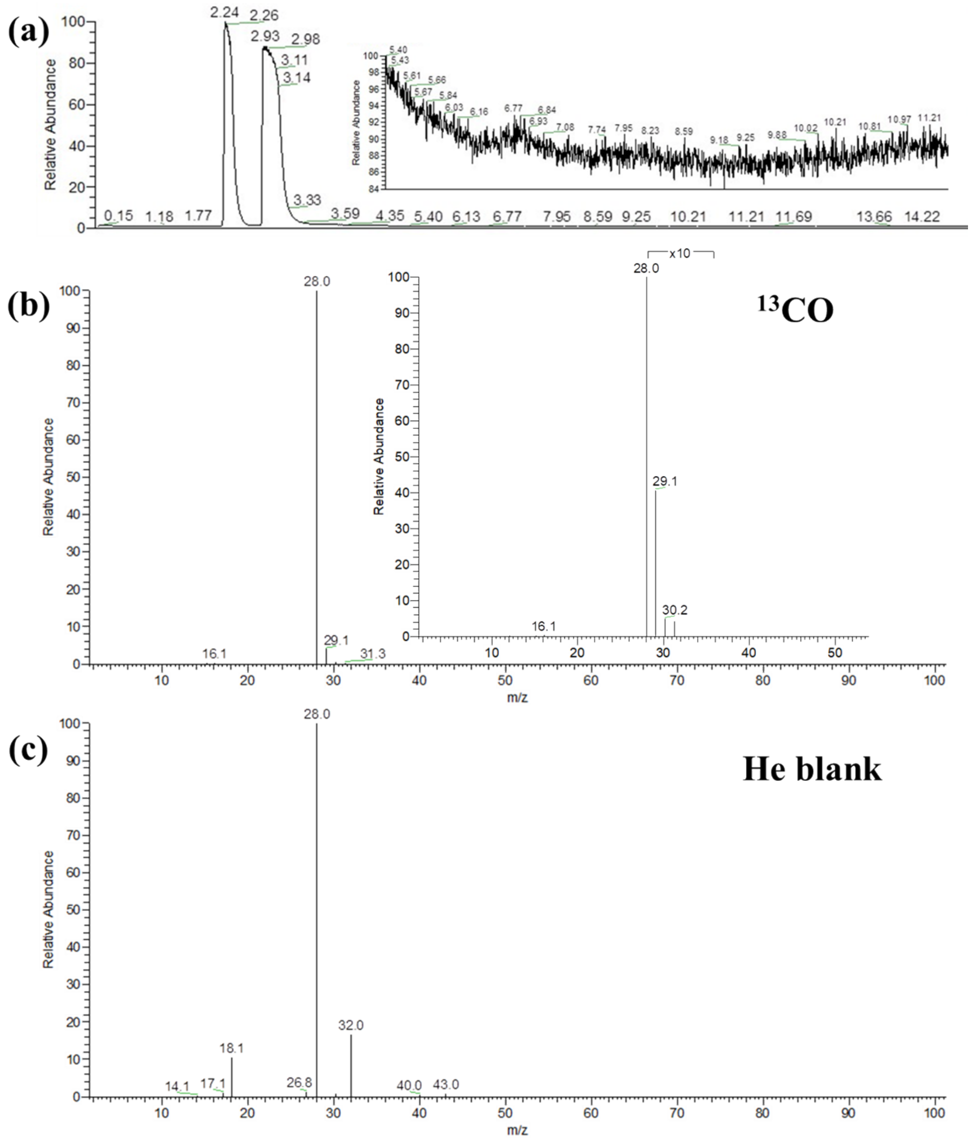

Figure S13. Total ion chromatography **(a)** and mass spectrum of **(b)** ^{13}C isotope tracing measurement in CO_2 photoreduction over 1.5Fe-Bi_2WO_6 (the inset figures show the zoom region of ^{13}CO peak) **(c)** He blank test.

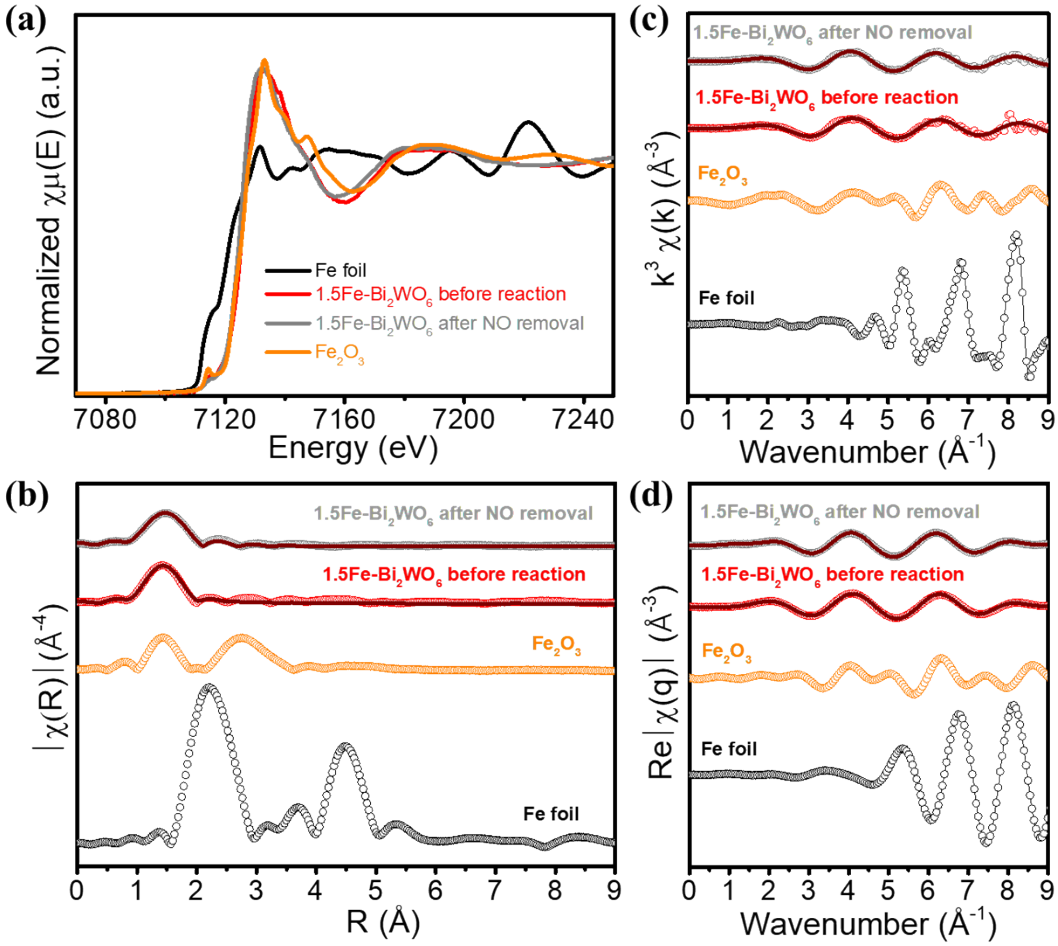

Figure S14. **(a)** Fe K-edge XANES, **(b-d)** FT-EXAFS spectra and corresponding fitting curves of Fe foil, Fe_2O_3, and 1.5Fe-Bi_2WO_6 before and after stability test for photocatalytic NO removal.

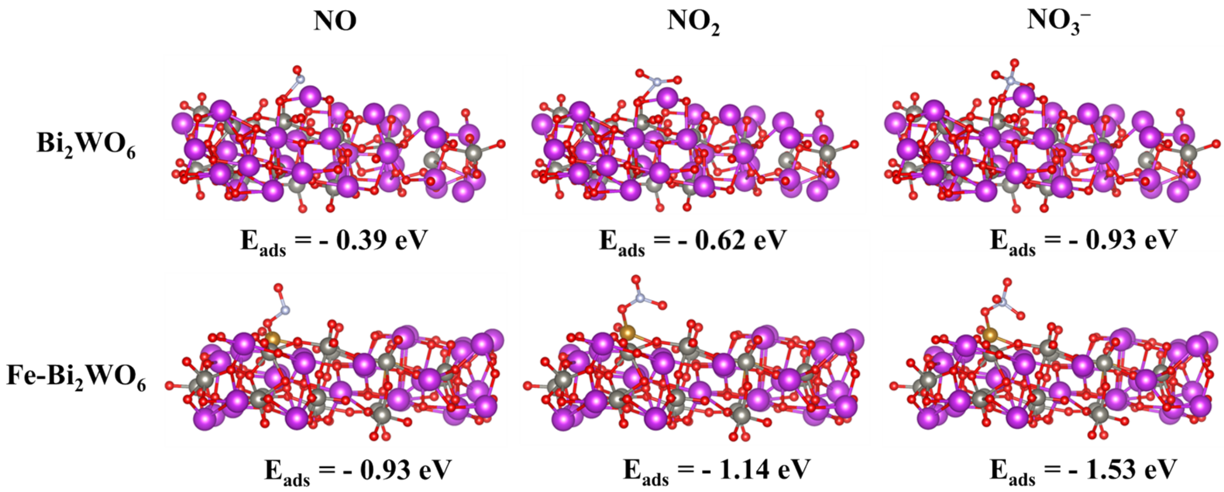

Figure S15. The adsorption energy of NO, NO_2, and NO_3^- during photocatalytic NO removal on Bi_2WO_6 and Fe-Bi_2WO_6 (131).

Table S1. The Fe content of Fe-Bi_2WO_6 samples was measured by ICP-OES.

Samples	**1Fe-Bi_2WO_6**	**1.5Fe-Bi_2WO_6**	**2Fe-Bi_2WO_6**
Fe amount (wt.%)	0.06	0.11	0.18

Table S2. Computed average bond lengths (d) of pristine Bi_2WO_6 and Fe-Bi_2WO_6

	d (Å)	
	Bi-O	**W-O (Fe-O)**
Bi_2WO_6	2.295	1.864
Fe-Bi_2WO_6	2.268	1.872 (1.898)

Table S3. BET surface area, pore volume, and pore diameter of Bi_2WO_6 and xFe-Bi_2WO_6 (x=1, 1.5, 2).

Catalysts	BET surface area ($m^2\ g^{-1}$)	Pore volume ($cm^3\ g^{-1}$)	Pore diameter (nm)
Bi_2WO_6	70.37	0.32	8.13
1Fe-Bi_2WO_6	104.93	0.40	5.08
1.5Fe-Bi_2WO_6	106.33	0.41	6.82
2Fe-Bi_2WO_6	105.68	0.42	4.46

Table S4. Structural parameters of x$Fe-Bi_2WO_6$ (x=1, 1.5, 2) catalysts obtained from the EXAFS fitting.

	Scattering pair	**CN**	**R(Å)**	**σ^2**	**ΔE_0 (eV)**	**R-factor**
1$Fe-Bi_2WO_6$	Fe-O	4.06	2.01	0.0083	-1.58	0.0035
1.5$Fe-Bi_2WO_6$	Fe-O	4.11	1.99	0.0076	-3.27	0.0061
2$Fe-Bi_2WO_6$	Fe-O	4.18	1.99	0.0073	-3.34	0.0057

CN: coordination number; R: distance between the absorber and surrounding coordination atoms; σ^2: Debye-Waller factor to describe the variance due to the thermal and lattice disorder; ΔE_0: threshold energy correction; R-factor is used to assess the quality of fitting and the smaller value of R-factor the better fitting.

Table S5. Band levels (vs. vacuum level) were acquired from UPS and UV-Vis DRS results.

	Bi_2WO_6	1Fe-Bi_2WO_6	1.5Fe-Bi_2WO_6	2Fe-Bi_2WO_6
Work function	3.72	3.56	3.52	3.63
VBM	6.02	6.15	6.17	6.24
Band gap	2.88	2.77	2.74	2.69
CBM	3.14	3.38	3.43	3.55

* UPS spectra recorded with an incident photon energy of 21.2 eV.

Table S6. TRPL fitting parameters for Bi_2WO_6 and xFe-Bi_2WO_6 (x=1, 1.5, 2) samples, respectively.

Sample	τ_1 (ns)	A_1 (%)	τ_2 (ns)	A_2 (%)	τ_{ave} (ns)
Bi_2WO_6	0.27	24.25	1.53	75.75	1.46
1Fe-Bi_2WO_6	0.22	26.16	1.19	73.84	1.13
1.5Fe-Bi_2WO_6	0.21	22.79	1.12	77.21	1.07
2Fe-Bi_2WO_6	0.26	25.77	1.31	74.23	1.24

TRPL curves were fitted by bi-exponential decay function and the average lifetimes were calculated by the following **equation S1**:

$$\tau_{ave} = \frac{A_1.\tau_1^2 + A_2.\tau_2^2}{A_1.\tau_1 + A_2.\tau_2} \quad \textbf{(S1)}$$

Table S7. Structural parameters of 1.5Fe-Bi_2WO_6 before and after photocatalytic CO_2 reduction stability test acquired from the EXAFS fitting.

	Scattering pair	CN	R(Å)	σ^2	ΔE_0 (eV)	R-factor
1.5Fe-Bi_2WO_6 before reaction	Fe-O	4.11	1.99	0.0076	-3.27	0.0061
1.5Fe-Bi_2WO_6 after CO_2 reduction stability test	Fe-O	4.20	1.99	0.0072	-1.63	0.0024

Table S8. Comparison of the photocatalytic CO_2 reduction yield of previously reported studies and our catalyst.

Materials	Reaction conditions	Products	Yield of CO_2 reduction ($\mu mol \cdot g^{-1} \cdot h^{-1}$)	Ref.
Bi_2WO_6/TiO_2 heterostructures	• Flow type • UV illumination	CH_4	1.06	[1]
Atomically thin Bi_2WO_6 nanosheets with hydrophobic and nonpolar surface	• Flow type • A 300 W Xe lamp	CO	7.12	[2]
		CH_4	0.63	
Chloride Modified Bi_2WO_6 Nanosheets	• Flow type • 300 W Xenon lamp	CO	1.66	[3]
		CH_4	0.35	
2D/2D Bi_2WO_6/BiOI heterojunctions	• Flow type • 500 W Xenon arc lamp with an UV cut-off filter	CH_4	2.29	[4]
2D/2D MXene/Bi_2WO_6	• Batch type • A Xe lamp	CH_4	1.78	[5]
		CH_3OH	0.44	
Atomically dispersed Fe-Bi_2WO_6	• Batch type	CO	9.20	**This study**

Table S9. Structural parameters of 1.5Fe-Bi_2WO_6 before and after photocatalytic NO removal stability test acquired from the EXAFS fitting.

	Scattering pair	CN	R(Å)	σ^2	ΔE_0 (eV)	R-factor
1.5Fe-Bi_2WO_6 before reaction	Fe-O	4.11	1.99	0.0076	-3.27	0.0061
1.5Fe-Bi_2WO_6 after NO removal stability test	Fe-O	4.18	1.99	0.0073	-3.34	0.0057

Table S10. Comparison of the photocatalytic NO removal efficiency, the selectivity of the NO_3^- product of previously reported studies and our catalyst.

Materials	Catalyst's dosage	NO conc. (ppb)	Light source	NO removal efficiency (%)	NO_2 conversion efficiency (%)/(ppb)	NO_3^- selectivity (%)	NO removal stability (%)	Ref.
Oxygen vacancies modified Bi_2WO_6	0.2	550	Visible light	47	-	-	Loss of 10% after 5 cycles	[6]
$Bi_{12}GeO_{20}$-Bi_2S_3	0.4	580	Visible light	46	> 5 ppb	96	-	[7]
Ternary Bi/Bi_2O_3/Bi_2WO_6 composite	0.2	550	Visible light	55.4	-	-	-	[8]
Carbonate-intercalated defective Bi_2WO_6	0.2	550	Visible light	55	-	-	Loss of ~13% after 5 cycles	[9]
Fe(iii) cluster-grafted $(BiO)_2CO_3$	0.1	550	Visible light	44.1	-	-	-	[10]
Bi_2WO_6/BiOI heterostructure	0.2	500	Visible light	40	-	-	-	[11]
Atomically dispersed Fe-Bi_2WO_6	0.2	500	Visible light	50.4	0.37%/ < 2 ppb	99.6	Loss of 4.3% after 5 cycles	**This study**

(-) means did not mentioned or state the specific numbers.

Reference

1. L. Collado, M. Gomez-Mendoza, M. García-Tecedor, F. E. Oropeza, A. Reynal, J. R. Durrant, D. P. Serrano and V. A. de la Peña O'Shea, *Applied Catalysis B: Environmental*, 2023, **324**, 122206.
2. Y. Liu, D. Shen, Q. Zhang, Y. Lin and F. Peng, *Applied Catalysis B: Environmental*, 2021, **283**, 119630.
3. Y. Y. Li, J. S. Fan, R. Q. Tan, H. C. Yao, Y. Peng, Q. C. Liu and Z. J. Li, *ACS Appl Mater Interfaces*, 2020, **12**, 54507-54516.
4. X. Y. Kong, W. Q. Lee, A. R. Mohamed and S.-P. Chai, *Chemical Engineering Journal*, 2019, **372**, 1183-1193.
5. S. Cao, B. Shen, T. Tong, J. Fu and J. Yu, *Advanced Functional Materials*, 2018, **28**, 1800136.
6. W. C. Huo, X. a. Dong, J. Y. Li, M. Liu, X. Y. Liu, Y. X. Zhang and F. Dong, *Chemical Engineering Journal*, 2019, **361**, 129-138.
7. F. Chang, X. Wang, C. Yang, S. Li, J. Wang, W. Yang, F. Dong, X. Hu, D.-g. Liu and Y. Kong, *Composites Part B: Engineering*, 2022, **231**, 109600.
8. W. He, Y. Sun, G. Jiang, H. Huang, X. Zhang and F. Dong, *Applied Catalysis B: Environmental*, 2018, **232**, 340-347.
9. W. Huo, W. Xu, T. Cao, X. Liu, Y. Zhang and F. Dong, *Applied Catalysis B: Environmental*, 2019, **254**, 206-213.
10. X. Feng, W. Zhang, Y. Sun, H. Huang and F. Dong, *Environmental Science: Nano*, 2017, **4**, 604-612.

11. L. Wang, K. Xu, W. Cui, D. Lv, L. Wang, L. Ren, X. Xu, F. Dong, S. X. Dou, W. Hao and Y. Du, *Advanced Functional Materials*, 2019, **29**, 1808084.